Stability and electronic properties of SiGe-based 2D layered structures

2015 Mater. Res. Express 2 016301

(http://iopscience.iop.org/2053-1591/2/1/016301)

Materials Research Express

PAPER

Stability and electronic properties of SiGe-based 2D layered structures

RECEIVED
7 October 2014

ACCEPTED FOR PUBLICATION
1 December 2014

PUBLISHED
2 January 2015

Pooja Jamdagni[1], **Ashok Kumar**[2], **Anil Thakur**[3], **Ravindra Pandey**[4] **and P K Ahluwalia**[1]

[1] Department of Physics, Himachal Pradesh University, Shimla 171005, India
[2] Department of Physics, Panjab University, Chandigarh 160014, India
[3] Department of Physics, Govt. College Solan, Himachal Pradesh, 173212, India
[4] Department of Physics, Michigan Technological University, Houghton, Michigan 49931, USA

E-mail: j.poojaa1228@gmail.com **and** pk_ahluwalia7@yahoo.com

Keywords: siligene, DFT, mechanical strain, electronic structure, electric field

Supplementary material for this article is available online

Abstract

The structural and electronic properties of the in-plane hybrids consisting of siligene (SiGe), and its derivatives in both mono and bilayer forms are investigated within density functional theory. Among several pristine and hydrogenated configurations, the so-called chair conformation is energetically favorable for monolayers. On the other hand, the bilayer siligane (HSiGeH) prefers AB-stacked chair conformation and bilayer siligone (HSiGe) prefers AA-stacked buckled conformation. In SiGe, the Dirac-cone character is predicted to be retained. HSiGe is a magnetic semiconductor with a band gap of ∼0.6 eV. The electronic properties show tunability under mechanical strain and transverse electric field; (i) the energy gap opens up in the SiGe bilayer, (ii) a direct-to-indirect gap transition is predicted by the applied strain in the HSiGeH bilayer, and (iii) a semiconductor-to-metal transition is predicted for HSiGe and HSiGeH bilayers under the application of strain and electric field, thus suggesting SiGe and its derivatives to be a potential candidate for electronic devices at nanoscale.

1. Introduction

Two-dimensional (2D) nanostructures in the honeycomb lattice are currently materials of interest due to their unique electronic properties as compared to their bulk counterparts [1–5]. 2D hexagonal Si and Ge monolayers, referred to as silicene and germanene, respectively, are expected to be potential alternatives to graphene in the electronics industry [6]. As compared to sp^2 hybridization in graphene [7], a mixture of sp^2 and sp^3 hybridization in silicene [8] and germanene [9] induces a buckling that facilitates tuning of the band gap with relative ease by external means such as external electric field and mechanical strains [8–10].

In recent years, the possibility of fabricating van der Waals multilayer hetero-structures have yielded fascinating properties e.g. silicene/graphene nanocomposite induces the so called n-type and p-type doping of silicene and graphene, respectively [11], that can be controlled by interfacial spacing; the silicene/MoS_2 superlattice shows sizable band gap for fabrication of nanoscale devices based on silicone [12]; germanene/MoS_2 heterostructure opens up a small gap at Dirac point along with the retention of linear dispersion of bands due to germanene [13].

In addition to the out-of-plane heterostructures, the electronic properties of 2D materials can also be modified by making their in-plane hybrids. For example, the electronic and mechanical properties of in-plane graphene/hexagonal boron nitride (h-BN) are shown to be tunable by controlling the domain sizes from a few tens of nanometers to millimeters [14–16]. Note that graphene and h-BN have similar crystal structure with only 2% difference in their lattice constants.

The experimental feasibility to synthesize in-plane hybrid structures to tune the electronic properties triggered our interest in investigating the possibility of an in-plane hybrid structure of Si and Ge in the hexagonal lattice. Note that the electronic band structure of 2D materials can be manipulated by covalent bonding with

suitable atoms or groups of atoms [17, 18]. The simplest possibility is the full or partial hydrogenation of the lattice. Both 2D Si (silicene) and Ge (germanene) have buckled honeycomb structural geometry in their thermodynamically stable forms [8, 9, 19]. Considering that the difference between the lattice constant of silicene (3.86 Å) and germanene (4.0 Å) is only ~4% [20], synthesis of their lateral heterostructures can easily be achieved.

In the present work, the structural and electronic properties of mono and bilayer of the lateral hybrid structures of silicene and germanene named as 'siligene' are systematically investigated. Tuning of the electronic properties of siligene is further examined by applying external electric field and mechanical strain. Electronic properties of a fully hydrogenated graphane analogous of siligene named as 'siligane' and partially hydrogenated siligene referred to as 'siligone', in both mono and bilayer forms are also investigated under the effect of transverse electric field and mechanical strain. Note that the mechanical strength of the considered 2D structures is determined by the derived stress–strain relationship.

2. Computational method

Electronic structure calculations were carried out using density functional theory (DFT), pseudopotential and numerical atomic orbitals (NAOs) basis sets as implemented in SIESTA program package [21]. Local density approximation (LDA) within Ceperlay Alder (CA) parameterization was used for the exchange and correlation functional to DFT. Considering that GGA tends to overestimate the lattice constants, underestimating the cohesive energy and chemical bonding, the choice of LDA functional form in the present study sets up the upper limit for the predicted structural and electronic properties together with the mechanical strength of 2D structures [22].

The norm-conserving, relativistic pseudopotentials in fully separable Kleinman and Bylander form were used to treat electron–ion interactions [23]. The Kohn–Sham orbitals were expanded in a linear combination of numerical pseudoatomic orbitals using split-valance double-zeta with polarization (DZP) basis sets for all atoms. A 250 Ry mesh cutoff was used for reciprocal space expansion of the total charge density. The Brillioun zone was sampled by using $30 \times 30 \times 1$ Monkhorst–Pack of k-points. To avoid the interaction between the 2D system images, a vacuum distance of ~20 Å is used along z-direction. All calculated equilibrium configurations are fully relaxed, with residual forces less than 0.01 eV $Å^{-1}$.

3. Results and discussion

3.1. Structural properties

Siligene (SiGe) monolayer is predicted to be stable in a low-buckled configuration with the buckling parameter (Δ) of 0.58 Å which increases to 0. 72 Å for the bilayer SiGe (figures 1 and 2). This is in line with the results on the silicene bilayer whose buckling parameter is larger than that of the monolayer [8]. Note that SiGe monolayer is also predicted to be stable without negative frequencies in the previous study [24]. The equilibrium configurations of siligane (HSiGeH) and siligone (HSiGe) monolayer show ~0.15 Å higher buckling than the siligene monolayer (figure 1). Note that the buckling in the present context is the out-of-plane displacement of atoms from the planner geometry. The calculated lattice constant of SiGe monolayer is 3.95 Å, which is about the mean of the constituent lattice constants of 3.86 Å and 4.0 Å for silicene and germanene, respectively. The lattice constants of mono- and bilayers are found to remain nearly the same. The Si–Ge bond-length is 2.32 Å, which is in excellent agreement with previous studies based on DFT–LDA [19], DFT–GGA [24] and DFT–hybrid functional [25].

Our total energy calculations reveal the graphene-like planner structure of siligene (SiGe) to be +0.17 eV/atom higher in energy than low-buckled structure. A fully hydrogenated monolayer, siligane (HSiGeH) is found to be more stable in the chair conformation where hydrogen atoms are on alternating position on both sides of the plane. We find the configuration consisting of H on the same side of the plane, to be higher (~0.26 eV/atom) in energy. Semi-hydrogenated monolayer siligene (HSiGe) is more stable when H is attached to the Si atom (see supplementary information figure S1, available at stacks.iop.org/MRX/0/000000/mmedia).

Following the classification given for graphene and silicene, we consider the AB and AA types of stacking patterns for the SiGe bilayer. Our total energy calculations reveal that the AB-stacked bilayer is relatively more stable than the AA-stacked bilayer with the energy difference of about ~0.07 eV/atom. In the case of the bilayer siligane, twelve different configurations were considered for determination of its ground state depending upon the stacking patterns and the position of H-atoms (see supplementary information figure S2). The AB-stacked chair conformation is found to be most stable for the bilayer HSiGeH, while siligone (HSiGe) bilayer prefers AA-stacked buckled conformation in its ground state (see supplementary information figure S3).

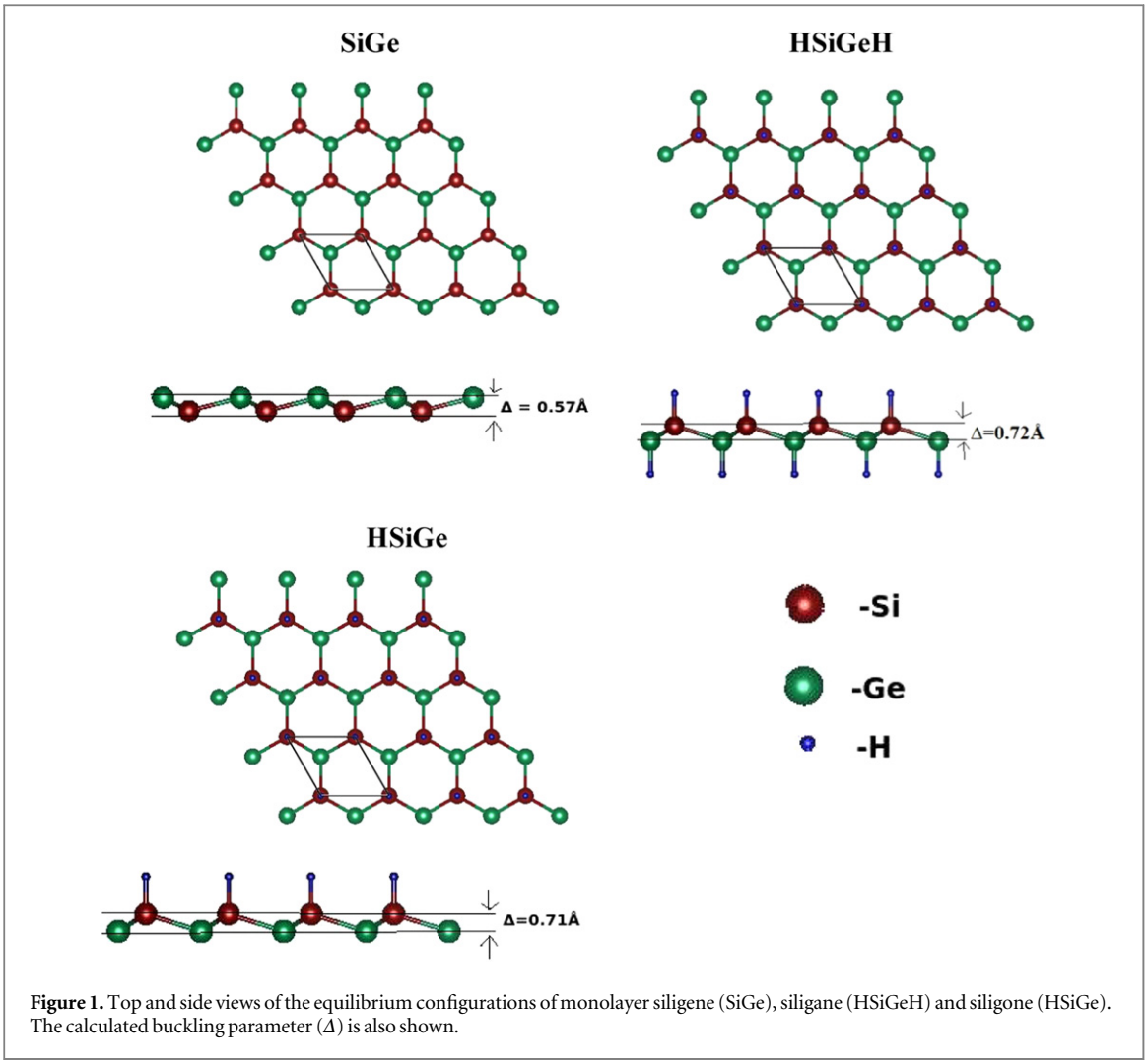

Figure 1. Top and side views of the equilibrium configurations of monolayer siligene (SiGe), siligane (HSiGeH) and siligone (HSiGe). The calculated buckling parameter (Δ) is also shown.

Total energy calculations show interlayer interaction in the siligane bilayer to be relatively weak ~ −0.02 eV/atom (table 1) as compared to those of siligene and siligone. The weak interaction in siligane bilayer is attributed to the steric hindrance between the hydrogen atoms of each layer that results in an increase in the interlayer separation to 3.92 Å from 2.49 Å of the siligene bilayer. The binding energy of siligene and siligone bilayer is calculated as −0.24 eV/atom and −0.50 eV/atom, respectively, which can be associated with the relatively strong covalent interactions between monolayers. Note that the binding energy for a bilayer system is calculated as the difference between the total energy of the bilayer system and the sum of the total energy of individual layers, while the formation energy of monolayer is calculated as the difference between the total energy of monolayer and the sum of the total energy of individual atoms. Negative signs of the binding energy and formation energy (table 1) represent the stability of the studied configurations.

3.2. Mechanical properties

The stress versus strain relationship provides a way to look at the mechanical properties of the materials under tensile strain. The maximum stress that a material can withstand while being stretched or pulled before breaking its sub-lattice symmetry gives its ultimate tensile strength and the maximum applied strain at which the breaking occurs is the ultimate tensile strain. The nano-indentation measurements have estimated the mechanical strength of monolayer graphene and MoS_2 to be 25% [26] and 11% [27], respectively.

The stress–strain relationship can be determined by calculating the stress tensor components in response to the strain tensor. The stress-tensor is defined as a positive derivative of the total energy with respect to the strain tensor [21, 28]. As the applied strain is biaxial and homogeneous, there is only one component of the stress tensor which gives the effective value of stress induced in 2D system in response to an applied strain. The maximum stress that is achieved in response to the tensile strain is calculated from the highest value of stress at which the slope becomes zero in the strain–stress curve. It is interesting to note that the fully hydrogenated SiGe (i.e. HSiGeH) shows the highest mechanical strength among monolayers, while semi-hydrogenated SiGe

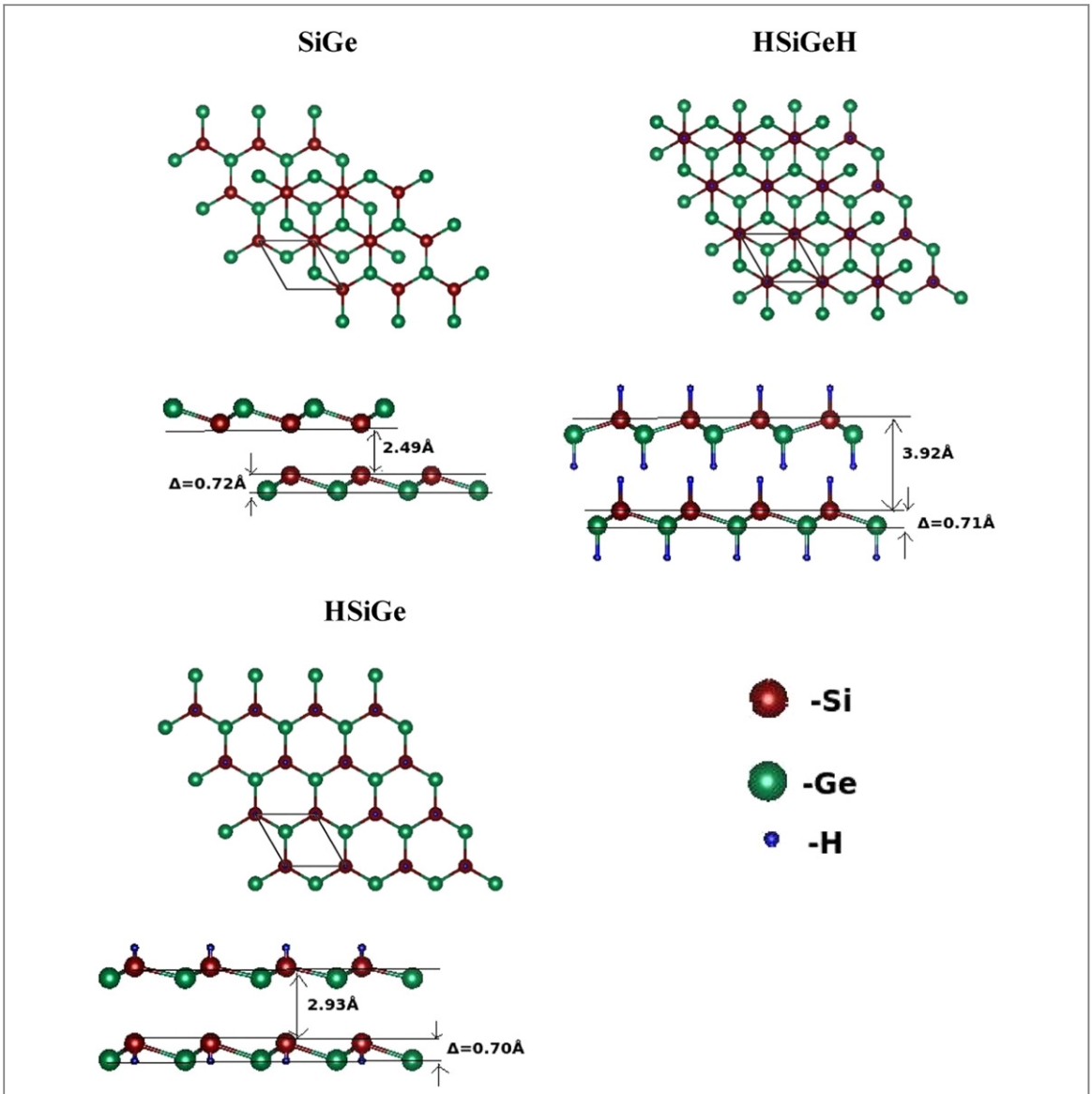

Figure 2. Top and side views of the equilibrium configurations of bilayer siligene (SiGe), siligane (HSiGeH) and siligone (HSiGe). The calculated buckling parameter (Δ) and interlayer distance are also shown.

Table 1. Buckling parameter (Δ), binding energy (E_b) of bilayers, formation energy (E_c) of monolayer, Si–Ge bond length (R_{Si-Ge}) and interlayer separation (h) of the SiGe, HSiGeH and HSiGe. The negative values of the binding and formation energy show the system to be stable.

	Siligene (SiGe)		Siligane (HSiGeH)		Silogone (HSiGe)	
	Monolayer	Bilayer	Monolayer	Bilayer	Monolayer	Bilayer
Δ (Å)	0.58	0.72	0.73	0.72	0.71	0.71
E_b (eV/atom)	—	−0.24	—	−0.02	—	−0.50
E_c (eV/atom)	−2.56	—	−2.76	—	−2.48	
R_{Si-Ge} (Å)	2.32	2.36	2.37	2.35	2.38	2.39
h (Å)	—	2.49	—	3.92	—	2.93

bilayers have highest mechanical strength among bilayers considered under tensile strain (figure 3). The ultimate tensile strength estimated for monolayer is about 2–3 GPa, while it is about 4–5 GPa for bilayers. The ultimate tensile strain is calculated as 16%, 20% and 20% (14%, 20% and 20%), respectively, for monolayers (bilayers) of siligene, siligane and siligone.

3.3. Electronic structure

The electronic band structures are calculated along the Γ–K–M–Γ directions of the Brillouin zone.

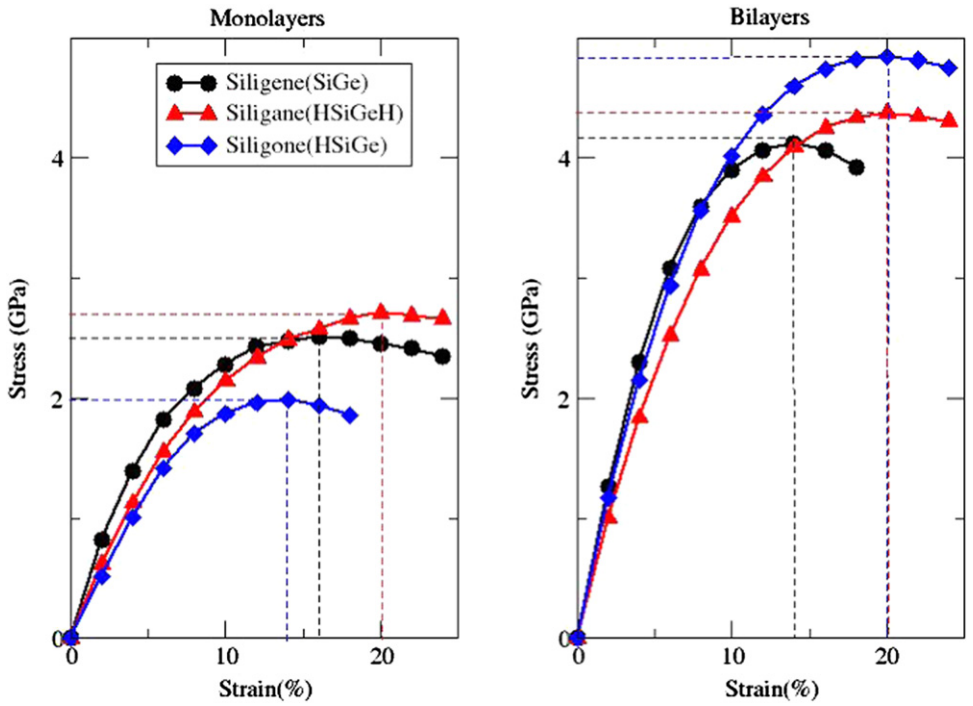

Figure 3. Stress versus strain curve for mono and bilayers of siligene, silagane and siligone. Ultimate tensile strain and strength are indicated by dotted lines.

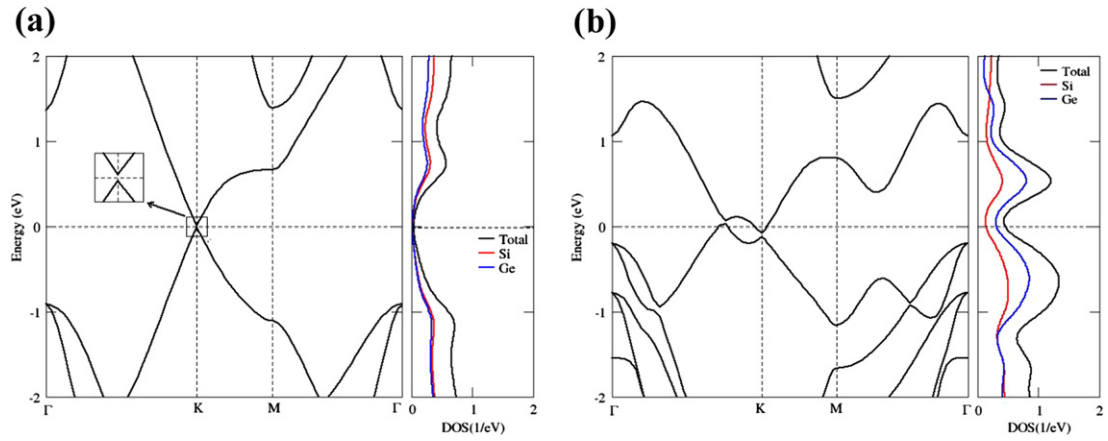

Figure 4. Electronic band structure and corresponding DOS of energetically favored structures of siligene (SiGe) monolayer (a) and bilayer (b). The Fermi-level is set at zero.

Similar to graphene [7], silicene [8] and germanene [9], a linear band dispersion with Dirac cone at 'K' is predicted for SiGe with the gap of 15 meV at Dirac point (figure 4(a)). The linear dispersion with Dirac cone at 'K' has also been reported previously [24]. The density of states (DOS) show equal contribution of Si and Ge atom in the vicinity of Fermi level that indicate the Dirac cone being a mixture of Si and Ge states. On the other hand, the energy band dispersion of bilayer SiGe resembles well with the bilayer silicene as far as the dispersion at 'K' and the K–Γ direction is concerned. Due to the buckled nature, SiGe bilayer consists of two Dirac cones (figure 4(b)) that crosses the Fermi level which is in contrast with the planner structure of bilayer graphene. DOS shows non-zero states at Fermi level that suggests the metallic nature of bilayer SiGe.

Siligane (HSiGeH), is predicted to be semiconductor (figure 5(a)) with a direct band gap of 2.05 eV at Γ" point. The band structure of bilayer siligane is similar to that of monolayer, except for the splitting of energy bands due to interlayer coupling (figure 5(b)) that results in the lowering of the energy gap to 1.85 eV. DOS calculations show the states around the Fermi energy are contributed by both Si and Ge atoms.

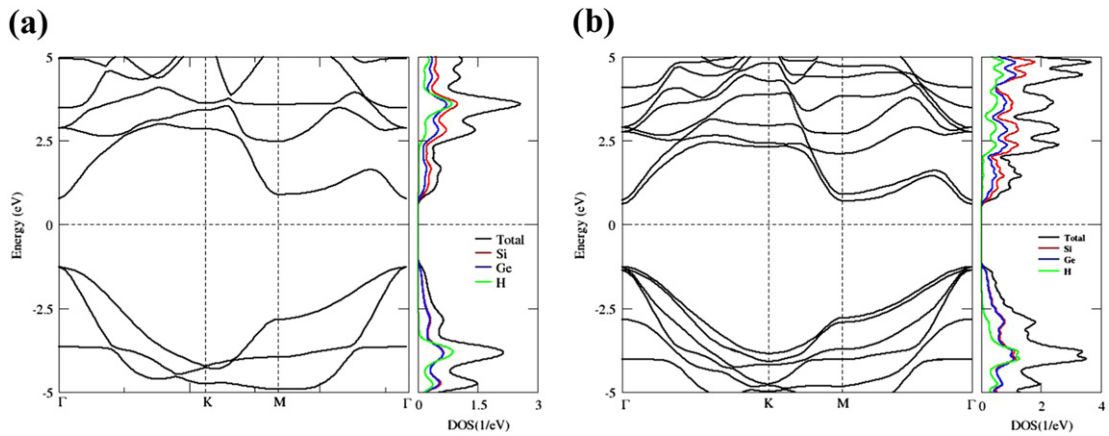

Figure 5. Electronic band structure and corresponding DOS of energetically favored structures of siligane (HSiGeH) monolayer (a) and bilayer (b). The Fermi-level is set at zero.

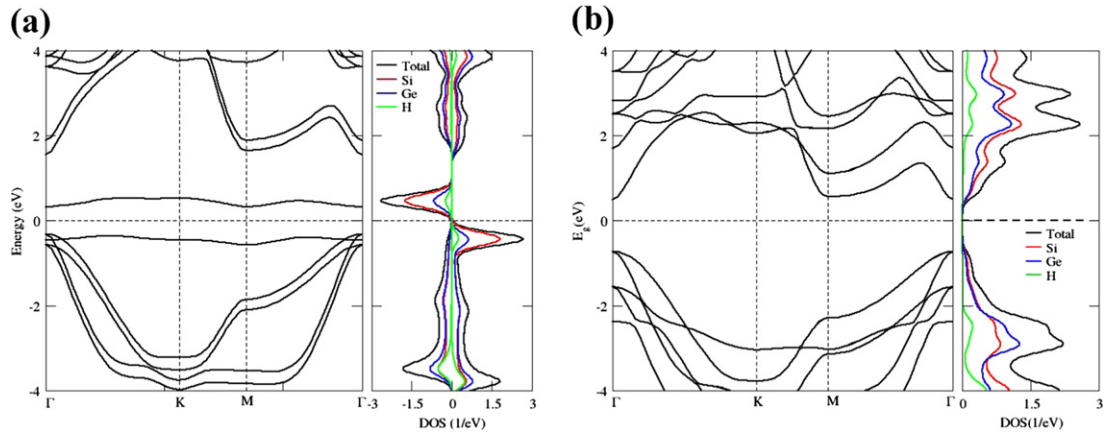

Figure 6. Electronic band structure and spin-polarized DOS of energetically favored structures of siligone (HSiGe) monolayer (a); band structure and corresponding DOS of most favored bilayer of siligone. The Fermi-level is set at zero.

Siligone (HSiGe), is a semiconductor and is magnetic in nature. The calculated band gap is 0.62 eV with the magnetic moment of $1\mu_B$. The magnetic moment is attributed to the odd number of electrons in HSiGe monolayer. The flat appearance of band gap near the Fermi level (figure 6(a)) indicates local magnetic moment formation in siligone. Magnetic nature of siligone also gets reflected from DOS where the difference in up and down spin states appears (figure 6(a)). On the other hand, siligone bilayer is a non-magnetic direct band gap semiconductor with 1.20 eV gap at 'Γ' (figure 6(b)). The non-magnetic behavior follows from an even number of unsaturated electrons in bilayer. The states near Fermi level are contributed by both Si and Ge atoms.

It is very important to mention here that the atomic arrangements of the constituent monolayers of a bilayer system have been found to strongly influence the electronic properties [29–31]. For e.g. band gap of bilayer graphane shows significant modulation on the flipping of one layer with respect to the other and by moving one layer along the diagonal of the other [29]. Also, the band gap in twisted bilayer graphene can be opened up as wide as 1.2 eV by interlayer covalent interactions in certain hydrogenation patterns [30]. However, we have not considered the twisting of one layer with respect to the other in bilayer systems.

3.4. Effect of mechanical strain and external electric field

Earlier studies have shown that the mechanical strains and external electric field are a powerful tool to engineer the electronic properties of the nanostructures [7, 8, 10, 32–37]. For example, the band gap in silicene can be opened to some meV by applying mechanical strain and external electric field [8, 10, 33]; the electronic properties of germanane bilayer can be tuned from semi-metallic to metallic under transverse E-field [34]; the Dirac cone of graphene and its allotropes can be effectively tuned by mechanical strain [35, 36] for nanoelectronic applications etc The mechanical strains in the present calculations are applied as $e = \Delta a/a_0$, where

a_0 is equilibrium lattice constant and Δa is change in the lattice constant simulating the strain. The two type of in-plane strains namely biaxial tensile (+a+b) and compression (−a−b) were applied along x and y axis.

Mechanical strain and external electric field have significant impact on the electronic properties of siligene and its derivatives (figure 7, supplementary information figures S4–S9). The band gap at Dirac point opens up with small tensile and compression strain, while at higher strain the crossing of bands over Fermi level at 'Γ' point makes siligene monolayer into a metal (supplementary information figure S4). The band gap is found to open up by ∼20 meV and 55 meV for the applied tensile and compression strain, respectively. The external electric field also opens up the band gap ∼80 meV for 1 V Å^{-1} in siligene monolayer. On the other hand, tensile (compression) strain in bilayer siligene shifts energy bands towards (away from) the Fermi level at 'Γ' point by inducing the so called self-doping p-type (n-type) effect (supplementary information figure S5).

The effect of strain/field on band structure can also be depicted in terms of charge density difference profile which was calculated by subtracting the sum of the charge densities of each layer of bilayer system from the total charge density of the system. A small charge accumulates on Ge atoms when tensile strain is applied, while in the case of compression strain the charge accumulation occurs at Si atoms (see figures S10(b) and (c) of supplementary information). The external electric field does not show any effect at field <1 V Å^{-1} in terms of gap modulation, which gets also reflected in charge density difference profile that remains similar to the pristine one (figures S10(a) and (d) of supplementary information), however, small gap opening of about 40 meV at rather higher 1.5 V Å^{-1} field has been observed for bilayer when subject to the external field.

On the other hand, the semiconducting band gap 2.05 eV of monolayer siligane can be systematically reduced by both in-plane tensile and compression strain (see figure S6 of supplementary information). Increasing the magnitude of strain above a certain critical value transforms siligane into metal which is attributed to a significant redistribution of charge in charge density difference profile (see figure S11 of supplementary information). Note that charge density difference in a monolayer system was calculated by subtracting the sum of the charge density of individual atoms from total charge density of a monolayer. The transverse electric field does not have any effect on the energy-gap of siligane monolayer, which is attributed to the perfect symmetry of the monolayer structure, and is also reflected in the charge density difference profile where charge density difference of electrically gated monolayer remains similar to that of the pristine case (supplementary information figure S11(d)).

The electric field systematically reduces the energy-gap in the bilayer system by breaking inversion symmetry, and at certain high critical value of field a semiconductor-to-metal transition may occur (figure 7(b)). The direct band gap nature of both mono and bilayer siligane remain preserved till before they get transformed into metal, while direct-to-indirect band gap transition is seen in the case of compression strain. The change in the band gap is also evident in terms of significant redistribution of charge by the application of strain/field (supplementary information figure S12).

The semiconductor-to-metal transition also occurs for siligone monolayer, however, at small value of about ∼4% for compression strain and of about ∼8% for tensile strain (figure 7(c)), which is understandable in terms of bridging a small band gap of 0.6 eV for the monolayer. In contrast to fully hydrogenated siligene monolayer (HSiGeH), the semi-hydroginated siligene (HSiGe) monolayer responds to the transverse electric field (figure S8). The closing of the band gap also happens for bilayer siligone by the applied mechanical strain, while it remains robust for the external field in terms of a change in the band gap (figure S9, supplementary information), which may be due to the large covalent interactions ∼ −0.5 eV/atom between the layers of siligone.

3.5. Deformation potentials

The change in the energy band as a function of applied strains can be quantified in terms of deformation potential (DP) which is an essential parameter for device modeling [37, 38]. The change in the energy of valence band (conduction band) corresponding to per unit of strain is called valence band deformation potential (conduction band deformation potential). In the neighborhood of equilibrium lattice constant, the variation of energy bands for small strain is approximately linear and hence can be expressed as:

$$\Delta E_{VB} = DP_{VB} \times e \; \Delta E_{CB} = DP_{CB} \times e. \quad (1)$$

where $\Delta E_{VB}(\Delta E_{CB})$ is change in valance band (conduction band) energy, $e = \Delta a/a_0$ is the magnitude of strain and DP_{VB} (DP_{CB}) is the valance band deformation potential (conduction band deformation potential). The positive (negative) values of DP indicates shift in the energy band towards (away) from Fermi level on the application of strain. The relatively high value of DPs for siligane (table 2) reveals that mechanical strains modify its electronic structure at a significantly high rate.

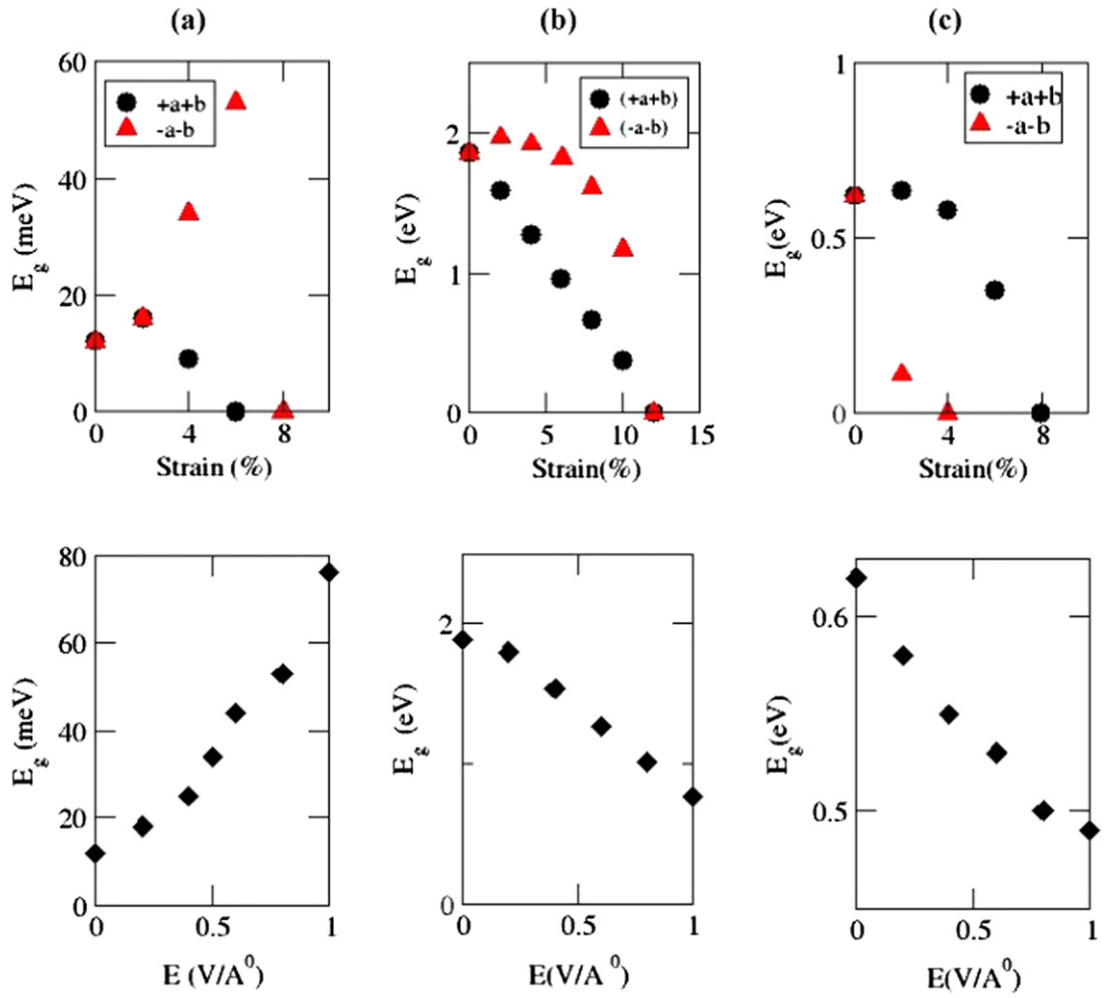

Figure 7. Band gap as a function of biaxial tensile (+a+b) and compression (−a−b) strain [upper panel]; band gap as a function of external electric field (E) [lower panel], for (a) monolayer siligene (b) bilayer siligane and (c) monolayer siligone.

Table 2. Valance band deformation potential (DP_{VB}) and conduction band deformation potential (DP_{CB}) in linear regime ($e < 2\%$) of biaxial tensile (+a+b) and compression (−a−b) strains applied to mono and bilayer of siligene, siligane and siligone.

		Siligene (SiGe)		Siligane (HSiGeH)		Siligone (HSiGe)	
		Monolayer	Bilayer	Monolayer	Bilayer	Monolayer	Bilayer
DP_{VB} (eV)	+a+b	−3.7	0.5	41.9	−19.5	−1.7	13.5
	−a−b	−3.8	1.0	−16.4	39.5	−10.8	3.4
DP_{CB} (eV)	+a+b	−3.3	0.3	−28.4	−36.4	1.2	12.2
	−a−b	−3.4	−0.2	−5.55	31.0	−9.4	−1.6

4. Summary

In summary, the structural and electronic properties of in-plane hybrids of hexagonal Si and Ge and their derivatives are studied. The interlayer interaction energy of siligane (HSiGeH) bilayer is found to be small as compared to the predicted strong covalent interactions between the layers of siligene (SiGe) and siligone (HSiGe) which is attributed to the strong steric hindrance effect due to hydrogen atoms in bilayer siligane. Siligane (HSiGeH) monolayer and siligone (HSiGe) bilayer are found to have highest mechanical strength under tensile strain among the studied configurations. Our studies show that magnetic moment can be induced in the monolayer by a controlled hydrogenation of the system. The electronic band gap can be induced and further modified by mechanical strain and transverse electric field thereby resulting in direct-to-indirect gap and semiconductor-to-metal transitions.

Our results are consistent with the fully and semi hydrogenated graphene [39, 40], e.g. electrically gated bilayer graphane has tunable band gap; graphone becomes a ferromagnetic semiconductor with small band gap; mechanical strain induces semiconductor-to-metal transition in graphane. We believe that strain engineering and electrical gating properties of the SiGe based hybrid structures can be exploited for applications in tunable nanoelectronic devices.

Acknowledgments

We gratefully acknowledge SIESTA team for code. PJ wishes to thank UGC-BSR New Delhi, India, for providing financial assistance in the form of a junior research fellowship. AK is thankful to UGC New Delhi, India, for financial support in the form of D S Kothari Post Doctoral Fellowship.

References

[1] Xu M, Liang T, Shi M and Chen H 2013 Graphene-like two-dimensional materials *Chem. Rev.* **113** 3766–98
[2] Butler S Z *et al* 2013 Progress challenges and opportunities in two-dimensional materials beyond graphene *ACS Nano* **7** 2898–926
[3] Kumar A and Ahluwalia P K 2013 Effect of quantum confinement on electronic and dielectric properties of niobium dichacogenides NbX_2 (X = S, Se Te) *J. Alloys Compd.* **550** 283–91
[4] Sharma M, Kumar A, Ahluwalia P K and Pandey R 2014 Strain and electric field induced electronic properties of two-dimensional hybrid bilayers of transition-metal dichalcogenides *J. Appl. Phys.* **116** 063711
[5] Kumar A and Ahluwalia P K 2012 Electronic structure of transition metal dichalcogenides monolayers 1H-MX_2 (M = Mo, W; X = S, Se, Te) *Eur. Phys. J.* B **85** 186
[6] Cahangirov S, Topsakal M, Akturk E, Sahin H and Ciraci S 2009 Two- and one-dimensional honeycomb structures of silicon and germanium *Phys. Rev. Lett.* **102** 236804
[7] Mohan B, Kumar A and Ahluwalia P K 2012 A first principle study of interband transitions and electron energy loss in mono and bi layer graphene: effect of external electric field *Physica* E **44** 1670–4
[8] Mohan B, Kumar A and Ahluwalia P K 2013 A first principle calculation of electronic and dielectric properties of electrically gated low-buckled mono and bilayer silicene *Physica* E **53** 233–9
[9] Kaloni T P and Schwingenschlogl U 2013 Stability of germanene under tensile strain *Chem. Phys. Lett.* **583** 137–40
[10] Mohan B, Kumar A and Ahluwalia P K 2014 Electronic and optical properties of silicene under uni-axial and bi-axial mechanical strains: a first principle study *Physica* E **61** 40–7
[11] Hu W, Li Z and Yang J 2013 Structural, electronic, and optical properties of hybrid silicone and germanene nanocomposite *J. Chem. Phys.* **139** 154704
[12] Li L and Zhao M 2014 Structures, energetics and electronic properties of multifarious stacking patterns for high-buckled and low-buckled silicene on the MoS_2 substrate *J. Phys. Chem.* C **118** 19129–38
[13] Li X, Wu S, Zhou S and Zhu Z 2014 Structural and electronic properties of germanene/MoS_2 monolayer and silicone/MoS_2 monolayer superlattices *Nanoscl. Res. Lett.* **9** 110
[14] Levendorf M P, Kim C-J, Brown L, Huang P Y, Havener R W, Muller D A and Park J 2012 Graphene and boron nitride lateral heterostructures for atomically thin circuitry *Nature* **488** 627–32
[15] Liu Z *et al* 2013 Raman, AFM and TEM characterization of graphene/h-BN interfaces *Nat. NanoTech.* **8** 119–24
[16] Fiori G, Betti A, Bruzzone S and Iannaccone G 2012 Lateral graphene-hBNC heterostructures as a platform for full two-dimensional transistors *ACS Nano.* **6** 2642–8
[17] Bianco E, Butler S, Jiang S, Restrepo O D, Windl W and Goldberger J E 2013 Stability and exfoliation of germanane: a germanium graphene analogue *ACS Nano.* **7** 4414–21
[18] Restrepo O D, Mishra R, Goldberger J E and Windl W 2014 Tunable gaps and enhanced mobilities in strain-engineered silicane *J. App. Phys.* **115** 033711
[19] Sahin H, Cahangirov S, Topsakal M, Bekaroglu E, Akturk E, Senger R T and Ciraci S 2009 Monolayer honeycomb structures of group-IV and III–V binary compounds: first-principles calculations *Phys. Rev.* B **80** 155453
[20] Lebegue S and Eriksson O 2009 Electronic structure of two-dimensional crystals from *ab initio* theory *Phys. Rev.* B **79** 115409
[21] Soler J M, Artacho E, Gale J D, Garc1ia A, Junquera J, Ordejon P and Portal D S 2002 The SIESTA method for *ab initio* order-N materials simulation *J. Phys.: Condens. Matter.* **14** 2745
[22] Li J, Medhekar N V and Shenoy V B 2013 Bonding charge density and ultimate strength of monolayer transition metal dichacogenides *J. Phys. Chem.* C **117** 15842−15848
[23] Troullier N and Martins J L 1991 Efficient pseudopotentials for plane-wave calculations. II. Operators fast iterative diagonalization *Phys. Rev.* B **43** 8861
[24] Zhou H *et al* 2013 First-principle prediction of a new Dirac-fermion material:silicon germanide monolayer *J. Phys.: Condens. Matter.* **25** 395501
[25] Suzuki T and Yokomizo Y 2010 Energy bands of atomic monolayers of various materials: possibility of energy gap engineering *Physica* E **42** 2820–5
[26] Lee C, Wei X, Kysar J W and Hone J 2008 Measurement of the elastic properties and intrinsic strength of monolayer graphene *Science* **321** 385–8
[27] Bertolazzi S, Brivio J and Kis A 2011 Stretching and breaking of ultrathin MoS_2 *ACS Nano.* **5** 9703–9
[28] Kumar A and Ahluwalia P K 2013 Mechanical strain dependent electronic and dielectric properties of two-dimensional honeycomd structure of MoX_2 (X = S, Se, Te) *Physica* B **419** 66–75
[29] Rohrer J and Hyldgaard P 2011 Stacking and band structure of van der Waals bonded graphane multilayers *Phys. Rev.* B **83** 165423
[30] Muniz A and Maroudas D 2012 opening and tuning of band gap by the formation of diamond superlattices in twisted bilayer graphene *Phys. Rev.* B **86** 075404
[31] Machado A, Maroudas D and Muniz A 2013 Tunable mechanical properties of diamond superlattices generated by interlayer bonding in twisted bilayer graphene *Appl. Phys. Lett.* **103** 013113

[32] Kumar A and Ahluwalia P K 2013 Semiconductor to metal transition in bilayer metals dichacogenides MX_2 *Model. Simul. Mater. Sci. Eng.* **21** 065015
[33] Ni Z, Liu Q, Tang K, Zheng J, Zhou J, Qin R, Gao Z, Yu D and Lu J 2012 Tunable bandgap in silicene and germanene *Nano. Lett.* **12** 113–8
[34] Li Y and Chen Z 2014 Tuning electronic properties of Germanane layers by external electric field and biaxial tensile strain: a computational study *J. Phys. Chem.* C **118** 1148–54
[35] Wang G, Si M, Kumar A and Pandey R 2014 Strain engineering of Dirac cones in graphyne *Appl. Phys. Lett.* **104** 213107
[36] Zhang Y B, Tang T T, Girit C, Zhao H, Martin M C, Zettl A, Crommine M F, Shen Y R and Wang F 2009 Direct observation of widely tunable bandgap in bilayer graphene *Nature* **459** 820–3
[37] Yan Q, Rinke P, Scheer M and Van de Walle C G 2009 Strain effects in group-III nitrides: defeormation potential for AlN, GaN, and InN *Appl. Phys. Lett.* **95** 121111
[38] Fishhetti M V and Laux S E 1996 Band structure, deformation potential, and carrier mobility in strained Si, Ge, and alloys *J. Appl. Phys.* **80** 2234
[39] Samarakoon D K and Wang X Q 2011 *Structural and Electronic Properties of Hydrogenated Graphene, Physics and Applications of Graphene—Theory* ed S Mikhailov (Rijeka: InTech)
[40] Zhang Y, Hu C-H, Wen Y-H, Wu S–Q and Zhu Z–Z 2011 Strain-tunable band gap of hydrogenated bilayer graphene *New J. Phys.* **13** 063047